

Dopamine drives left-hemispheric lateralization of neural networks during human speech

Stefan Fuertinger¹ | Joel C. Zinn² | Ashwini D. Sharan³ | Farid Hamzei-Sichani⁴ |
Kristina Simonyan^{5,6} 

¹Ernst Strüngmann Institute (ESI) for Neuroscience in Cooperation with Max Planck Society, Frankfurt, Germany

²Department of Neurology, Icahn School of Medicine at Mount Sinai, New York, New York

³Department of Neurosurgery, Sidney Kimmel College of Medicine, Thomas Jefferson University, Philadelphia, Pennsylvania

⁴Department of Neurosurgery, University of Massachusetts Memorial Medical Center, Worcester, Massachusetts

⁵Department of Otolaryngology, Massachusetts Eye and Ear Infirmary, Harvard Medical School, Boston, Massachusetts

⁶Department of Neurology, Massachusetts General Hospital, Harvard Medical School, Boston, Massachusetts

Correspondence

Kristina Simonyan, Department of Otolaryngology, Massachusetts Eye and Ear Infirmary, Harvard Medical School, 243 Charles Street, Suite 421, Boston, MA 02114.

Email: Kristina_Simonyan@meei.harvard.edu

Funding information

National Institute on Deafness and Other Communication Disorders, National Institutes of Health, Grant/Award Number: R01DC011805

Abstract

Although the concept of left-hemispheric lateralization of neural processes during speech production has been known since the times of Broca, its physiological underpinnings still remain elusive. We sought to assess the modulatory influences of a major neurotransmitter, dopamine, on hemispheric lateralization during real-life speaking using a multimodal analysis of functional MRI, intracranial EEG recordings, and large-scale neural population simulations based on diffusion-weighted MRI. We demonstrate that speech-induced phasic dopamine release into the dorsal striatum and speech motor cortex exerts direct modulation of neuronal activity in these regions and drives left-hemispheric lateralization of speech production network. Dopamine-induced lateralization of functional activity and networks during speaking is not dependent on lateralization of structural nigro-striatal and nigro-motocortical pathways. Our findings provide the first mechanistic explanation for left-hemispheric lateralization of human speech that is due to left-lateralized dopaminergic modulation of brain activity and functional networks.

KEYWORDS

fMRI, hemispheric lateralization, iEEG, neural modeling, speech production

1 | INTRODUCTION

Speech production is one of the most complex and unique human motor behaviors that dynamically engages over 100 orofacial, laryngeal and respiratory muscles. At the neural level, speech production is possible due to the orchestrated activation of multiple brain networks controlling sound perception, sensorimotor integration, and cognitive processing (Price, 2012; Fuertinger, Horwitz, & Simonyan, 2015; Simonyan & Fuertinger, 2015). A well-known and long-accepted hallmark of the organization of speech control is its left-hemispheric dominance, which is known since the time of Broca (Strauss, Kosaka, & Wada, 1983; Frost et al., 1999; Hull & Vaid, 2006). However, more

recent studies have argued for bilaterally balanced hemispheric involvement of large-scale functional networks during speaking and suggested that only particular sub-networks are left lateralized (Gehrig, Wibral, Arnold, & Kell, 2012; Cogan et al., 2014; Silbert, Honey, Simony, Poeppel, & Hasson, 2014; Simonyan & Fuertinger, 2015). Among these, the neural networks originating from the speech motor cortex (SMC) in the ventral sensorimotor cortex and the dorsal striatum were found to be prone to left-hemispheric lateralization (Simonyan, Ostuni, Ludlow, & Horwitz, 2009; Simonyan, Herscovitch, & Horwitz, 2013; Simonyan & Fuertinger, 2015). Adding to this growing body of literature, we recently demonstrated that speech-induced release of dopamine from substantia nigra, pars compacta (SNc), was lateralized to the left dorsal

striatum (Simonyan et al., 2013), whereas simulated dopamine release in the laryngeal motor cortex evoked pronounced changes in large-scale functional connectivity similar to that during real-life speech production (Furtinger, Zinn, & Simonyan, 2014). Nonetheless, a critical piece of the puzzle *explaining* direct dopaminergic modulation of motocortical neural activity during speech production and its potential influence on hemispheric laterality of neural networks remains missing. Specifically, it is unclear whether nigral phasic dopamine release drives or is being driven by left-hemispheric lateralization of motocortical and striatal networks while speaking.

To address these open questions, we examined the effects of dopaminergic neuromodulation on speech-related neural activity and functional networks across different spatial and temporal scales using a multi-modal analysis of functional MRI (fMRI) in combination with intracranial electroencephalography (iEEG) and a computational stochastic neural population and dopamine release model based on diffusion-weighted (DWI) MRI recordings. Based on available literature (Simonyan et al., 2013; Furtinger et al., 2014), we hypothesized that dopamine, as a major modulatory neurotransmitter, would directly influence motocortical and striatal neural activity, which would lead to left-hemispheric dominance of functional but not structural speech networks.

2 | MATERIALS AND METHODS

2.1 | Data acquisition and processing

Twenty right-handed monolingual English-speaking healthy subjects (13 females, 7 males, 55.2 ± 9.8 years) participated in the study. All subjects provided written informed consent prior to study participation, which was approved by the Institutional Review Boards of the Icahn School of Medicine at Mount Sinai, the Thomas Jefferson University, and National Institute of Neurological Disorders and Stroke, National Institutes of Health.

Functional MRI data were acquired on a 3T GE scanner (Milwaukee, WI) and included resting-state and sentence production paradigms as reported earlier (Simonyan et al., 2013; Furtinger et al., 2014; Simonyan & Fuertinger, 2015). Briefly, resting-state scans were acquired with a gradient-weighted echo planar imaging (EPI) pulse sequence (TR = 2 s, 150 contiguous volumes, TE = 30 ms, FA = 90 degrees, 33 slices with 3.75 mm in-plane resolution, slice thickness 4 mm), during which the participants laid still with their eyes closed in an environment with dimmed light. Subjects were continuously monitored during image acquisition, and no participant reported falling asleep in the scanner. Sentence production fMRI data were acquired with a gradient-weighted EPI pulse sequence (total TR = 10.6 s comprising 3.6 s delay for stimulus presentation, 5 s delay for task production, and 2 s image acquisition, TE = 30 ms, FA = 90 degrees, 36 slices with 3.75 mm in-plane resolution, slice thickness 4 mm) using a BOLD contrast with an event-related sparse-sampling design. Grammatically correct English sentences were acoustically presented one at a time and subsequently repeated by the subject one per acquisition volume. A total of 36 task-production trials and 24 resting fixations as a baseline were acquired

over five scanning sessions, with tasks pseudorandomized between sessions and participants. A high-resolution T1-weighted image was acquired as an anatomical reference using a magnetization-prepared rapid acquisition gradient echo (MPRAGE) sequence (TI = 450 ms, TE = 3.0 ms, FA = 10, 128 slices with 1.2 mm thickness).

All fMRI data pre-processing was performed using AFNI software (Cox, 1996) as reported earlier (Fuertinger et al., 2015; Simonyan & Fuertinger, 2015; Battistella, Fuertinger, Fleysler, Ozelius, & Simonyan, 2016). Resting-state data underwent anatomy-based correlation corrections (ANATICOR) to remove hardware-related noise (Jo, Saad, Simons, Milbury, & Cox, 2010). Physiological noise was removed using respiratory and cardiac signals synchronized with the EPI data based on retrospective image correction (RETROICOR) (Glover, Li, & Ress, 2000). Residual time-series were spatially smoothed within the gray matter using a 6-mm Gaussian kernel and normalized to the AFNI standard Talairach-Tournoux space. Multiple linear regression analyses with a single regressor for the task convolved with the canonical hemodynamic response function were performed to assess speech-related brain activity. Following two empirical studies (Desikan et al., 2006; Hagmann et al., 2008), the whole brain was parcellated into 70 regions of interest (ROIs), comprising 64 cortical and 6 subcortical areas. Using this parcellation, regionally averaged speech-production and resting-state BOLD fMRI residual time-series were extracted for all subjects (Furtinger et al., 2014).

Whole-brain diffusion-weighted images were acquired with a single-shot spin-echo EPI sequence (TE = 80 ms, TR = 8.9 s, FOV = 240 mm, matrix 120×118 mm, 68 contiguous slices, slice thickness 2 mm) using 60 noncolinear directions with a b-factor of $1,000 \text{ s/mm}^2$. The DWI data were processed using the same 70 ROIs in the FATCAT Toolbox of AFNI following standard processing steps (Taylor & Saad, 2013). Based on the resultant tractography data, a group-averaged 70×70 structural connectivity matrix was constructed and normalized with respect to its largest row-sum and formed the anatomical coupling matrix for our neural population model. To estimate the extent to which simulated functional lateralization might be driven by hemispheric differences in structural connectivity, we analyzed the laterality footprint of the employed coupling matrix. We computed the fiber count (number of non-zero elements) and the connection strength for each hemisphere. Both the number of fibers (left: 690, right: 659) and their corresponding connection weights (left: 0.41 ± 0.34 , right: 0.37 ± 0.34 , $p = .61$, two-sample t test at $p < .05$) demonstrated hemispheric balance of the employed coupling matrix. This implies that simulated functional lateralization effects were not a mere consequence of hemispheric differences in structural connectivity.

Sixteen iEEG recordings, including eight resting-state and eight speech production segments, were obtained from patients undergoing subdural iEEG recordings for epileptic seizure monitoring. Seizure foci were localized in the rostral frontal and occipital regions and, thus, were spatially separated from motor cortical areas not influencing the SMC region, from which recordings were analyzed in this study. All iEEG time-series were recorded from subdural grid electrodes with center-to-center distances of 10 mm (Integra, Plainsboro, NJ) and a

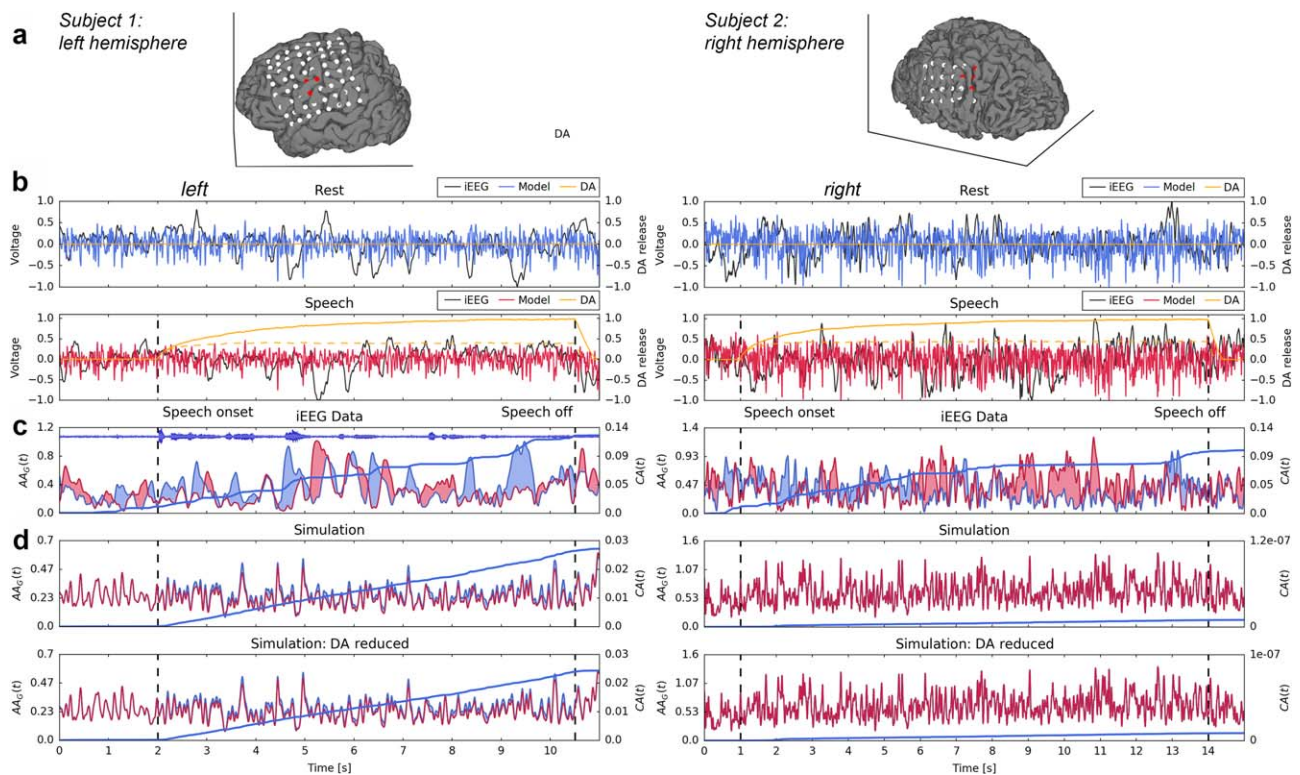


FIGURE 1 Neural activity in the speech motor cortex measured by iEEG recordings and predicted by the model at rest and during speech production. (a) Relative location of surgically placed subdural electrodes on the cortical surface in the standard Montreal Neurological Institute (MNI) space in Subject 1 (left) and Subject 2 (right). Electrodes covering the speech motor cortex are shown in red. (b) Simulated excitatory membrane potentials at rest (blue) in the left and right speech motor cortex under tonic dopamine (DA) levels (orange) with resting state iEEG signals averaged across three electrodes above the left speech motor cortex in Subject 1 (left), and four electrodes recording from the right speech motor cortex in Subject 2 (right) overlaid in black. The second panel uses the same format to illustrate simulated neural potentials (red) modulated by normal (solid orange) and 50% reduced phasic dopamine (dotted orange) with speech production iEEG data shown in black. (c) Temporal evolution of smooth envelopes (AA_G) corresponding to iEEG recordings at rest and while speaking. Areas where resting state $AA_G >$ speech production AA_G are shaded in blue, otherwise areas are shaded in red with the overlaid blue line showing the corresponding CA curve. The waveform of the audio signal extracted from video recording corresponding to the analyzed iEEG segment is overlaid on top. Panel (d) uses the same format as (c) to show AA_G and CA curves based on simulations using normal (top) and 50% reduced (bottom) phasic dopamine levels. All plots are based on the same resting state and speech production segments (per subject). Similar patterns were observed in all other recordings

surface diameter of 2.5 mm with a sampling rate of 1 kHz per channel (Nihon Kohden America, Irvine, CA). To determine exact electrode locations relative to motocortical regions in standard space, imaging data were transformed to the Montreal Neurological Institute (MNI) space using a surface-based co-registration (Fischl, Sereno, Tootell, & Dale, 1999) with the MNI305 average brain. The resulting deformation field was subsequently used to map Cartesian electrode coordinates from the subject's native surface space onto the average pial surface (Dykstra et al., 2012). In addition, direct cortical stimulation mapping localized the sensorimotor cortex in relation to electrode placement. Based on both registered coordinates in standard space and cortical stimulation mapping, we localized the electrodes within the 8×8 grid that covered the SMC, including the laryngeal and orofacial representations as described previously (Bouchard, Mesgarani, Johnson, & Chang, 2013; Simonyan, 2014) (Figure 1a).

Speech production segments were 60 seconds in length and consisted of uninterrupted natural speaking as part of a conversation. Each

speech segment contained one second of silent (non-speech) activity at the beginning and the end. Resting-state periods were chosen to match the duration of speech segments. All segments were selected with maximal temporal distance (2–24 hr) from a clinical and/or electrographic seizure episode to ensure that recordings were not confounded by seizure activity. To assess the quality of iEEG signals, each time-course was visually screened for acquisition artifacts and excessive noise.

2.2 | Neural modeling

We used a physiologically informed non-linear large-scale multi-compartment neural population model as described previously (Fuertinger et al., 2014) that simulated brain activity during the resting state and speech production. Briefly, the model was based on coupled small-scale local sub-models that each represented neural activity within one of the 70 ROIs defined by the employed parcellation (see Data

Acquisition and Processing). Each regional subsystem was composed of connected mean field models of excitatory and inhibitory neurons, whose dynamics were governed by voltage-gated potassium, sodium, calcium, and leaky ion channels (Breakspear, Terry, & Friston, 2003). Thus, the full model was given by a system of 140 coupled non-linear stochastic differential equations that simulated population-averaged membrane potential dynamics. A rigorous mathematical proof establishing existence and uniqueness of solutions to the used model as well as a computationally efficient strategy to numerically approximate these solutions can be found in (Furtinger et al., 2014).

In the current study, the developed dopamine release model was extended to not only reflect the direct dopaminergic pathway between substantia SNc and SMC, which comprises the laryngeal and orofacial representations (Bouchard et al., 2013; Simonyan, 2014), but also to include SNc-putamen projections as part of the direct dopamine release pathway. We demonstrated in an earlier study that speech production was associated with left-striatal release and binding of endogenous dopamine (Simonyan et al., 2013). Based on these findings, we simulated speech production via phasic dopamine release within the left nigro-striatal as well as nigro-cortical pathways. Keeping bilateral dopamine release at tonic levels simulated the resting-state condition.

We accounted for inter-subject variability by matching each empirical study participant with a virtual subject, created by using a fixed but arbitrary random number generator seed to sample inhibitory-to-excitatory and non-specific-to-excitatory synaptic coupling strengths a_{ie} and a_{ne} , respectively, as well as the Wiener process in the stochastic differential equation system.

To quantify the contribution of structural connections to differences seen in hemispheric activation patterns, we performed a second set of simulations, for which structural connections between left SNc and SMC as well as left SNc and putamen were artificially strengthened by doubling the corresponding entries in the employed coupling matrix. This modified coupling matrix was subsequently used in the same (and otherwise unchanged) virtual subjects to repeat resting-state and speech production simulations.

To adequately reflect neural dynamics captured by iEEG recordings, we did not only adjust the length of simulations but also matched endogenous dopamine release with speech timing. We further assessed the impact of dopaminergic neuromodulation on functional lateralization by performing two simulations corresponding to each empirical recording to mimic normal dopamine levels as well as a 50% decrease in available phasic dopamine. It has been shown that healthy aging leads to an almost linear decline in available striatal dopamine of around 46% over an age range of 70 years (van Dyck et al., 2002). Thus, to simulate age-related dopamine deficiencies and analyze their effect on lateralization patterns, phasic dopamine levels were artificially halved by reducing the maximum dopamine production rate in the model, r_{max} . To further assess the effect of dopamine availability on hemispheric dominance patterns, we performed simulations corresponding to increases and reductions in phasic dopamine from $0 \pm 100\%$ (10% steps) of its default level.

2.3 | Quantification of laterality in simulated and empirical fMRI

Lateralization of simulated and empirical fMRI signals in the resting state and during speech production was estimated by using three types of laterality indices (see Appendix for computational details). We first considered whole-brain activity and as a second step focused on speech-related sub-networks. As a first step, we used a traditional laterality index, Ll_1 , based on the L^1 -norm of regional activity (Seghier, 2008). While this index is straightforward to compute, its interpretation relies on a number of methodological factors like the definition of a proper hemispheric dominance threshold (Baciu et al., 2001), choice of a baseline condition (Newman, Twieg, & Carpenter, 2001), or ROI selection (Spreer et al., 2002). The significance of lateralized activation patterns, and thus indirectly a hemispheric dominance threshold, was not determined using a fixed cutoff value but instead via statistical testing as detailed below. To incorporate a subject-specific baseline condition, we additionally calculated a task-based laterality index, Ll_t , adjusted for resting-state activity (see Appendix).

To analyze the effect of speech-driven activity changes on the functional profile of specific speech-related regions, a psychophysiological interaction (PPI) analysis (Friston et al., 1997) was performed. Following the employed dopamine release model, we chose the bilateral SMC, SNc, and putamen (PUT) as seed regions. The corresponding resting-state and speech-production time-series were multiplied by the associated task vector and regressed with the whole brain. A p -value $\leq .05$ was set as indicative of significant speech-driven changes in functional connectivity of a region with the seed. Lateralization patterns of these seed-based speech-related sub-networks were quantified by adapting Ll_t in the following manner. For each seed, Ll_t (SMC_L), Ll_t (SMC_R), Ll_t (PUT_L), Ll_t (PUT_R) were calculated respecting only ROIs with $p \leq .05$. Thus, to gain a comprehensive overview of language laterality we analyzed (a) raw whole-brain values of Ll_1 at rest and during speech production, (b) baseline-corrected Ll_t , and (c) localized, baseline-corrected PPI-based Ll_t .

2.4 | Quantification of laterality in iEEG and simulated neural potentials

We used a simulation-aided approach to quantify lateralization in subdural iEEG recordings. High-gamma bands have been reported to be robust neural correlates of local neural activity in speech and language tasks (Towle et al., 2008; Chang et al., 2011), while slow oscillations have been implied in cognitive processing and word production (Llorens, Trebuchon, Liegeois-Chauvel, & Alario, 2011). To reflect cortical oscillations at different states of synchrony, we applied a 0.1–200 Hz broad-band filter to both recordings and simulations (Gow, Keller, Eskandar, Meng, & Cash, 2009). Comparability of model output and data recordings was further facilitated by averaging iEEG signals across the respective electrodes of interest, after which both simulations and data were de-meaned and amplitude-normalized to the range $[-1, +1]$ to account for scale differences.

To analyze the frequency-dependence of oscillation amplitudes in simulations and iEEG recordings, we assessed the power spectral density (PSD) of computer-generated and empirical signals using Welch's estimation strategy (Welch, 1967) to compute sliding periodograms based on 2s-Hanning windows with 25% overlap. Additionally, we employed the same strategy to calculate the average cross-spectral density between data and simulations at rest and during speech production, respectively, to estimate the cross-covariance of frequencies found in recordings and generated by the model during both conditions. Following the rationale that amplitude patterns as revealed by signal envelopes are correlated with intentional behavior (Freeman, 2005), we calculated smooth envelopes AA_G of data recordings and simulations (see Appendix). To quantify a potential reduction in speech-production signal amplitudes with respect to a resting-state baseline as observed in recent empirical studies (Lachaux et al., 2007; Flinker et al., 2015), we calculated the cumulative difference CA of the corresponding smooth envelopes.

2.5 | Statistical evaluation of laterality in simulated and empirical fMRI

The statistical analysis was based on a two-tiered approach. First, we performed linear mixed effect (LME) model analyses to assess the statistical dependence of simulated and empirical laterality index values on the experimental condition (resting state or speech production). Specifically, we constructed two LME models to separately analyze simulations and recordings. In both models, experimental condition and laterality index type (LI_1 , LI_r , PPI-based LI_t) were used as interacting fixed effects with an intercept for (virtual) subjects as random effect. Experimental condition was a two-level factor for empirical recordings (with levels resting state and speech production) but comprised four levels for simulations to account for results based on enhanced structural coupling. To assess whether lateralization differences were related to the observed condition, we performed likelihood ratio tests of the constructed models against corresponding null models without experimental condition as fixed effect at a corrected $p \leq .05$. In the same manner, we assessed whether the constructed models differed significantly from associated models without an interaction term for experimental condition and laterality index type to assess the significance of this interdependence. In a post-hoc analysis, both models were subjected to simultaneous two-sided general linear hypotheses testing of least squares means to assess differences in laterality index values related to experimental condition (and structural coupling) at $p \leq .05$, adjusted for multiple comparisons.

In a second step, we analyzed differences in laterality index values across empirical recordings and simulations using a linear model with index origin (simulation or recording) and index type as interacting fixed effects. This model was similarly subjected to likelihood ratio tests to assess the statistical significance of this interaction as well the dependence of index values on their respective origin (see Appendix for details).

2.6 | Statistical evaluation of laterality in iEEG and simulated neural potentials

To quantify the extent of similarity in simulated and empirical signal amplitudes with respect to the corresponding resting-state baselines, we correlated the associated ipsilateral CA curves. For this, we calculated Pearson correlation coefficients between left SMC voltages predicted by the model corresponding to normal and artificially reduced phasic dopamine levels and CA curves based on left-sided electrodes and vice versa. Additionally, we performed a simulation-aided analysis of real-time dopaminergic modulation on lateralization patterns in iEEG recordings by correlating normal and reduced in silico dopamine release patterns in the left SMC with corresponding empirical CA curves.

In a follow-up analysis, we used LME modeling to assess whether changes in the calculated correlations were related to either the observed hemisphere (left or right) or phasic dopamine release level (normal or reduced), respectively. Thus, we constructed two LME models to separately analyze CA - CA and dopamine- CA correlation coefficients, respectively, which were converted to Z-scores using Fisher's Z-transform. We used hemisphere and phasic dopamine release level as interacting fixed effects and an intercept for (virtual) subjects as random effect in both models. Likelihood ratio tests were employed to assess the significance of fixed effect interactions. Similarly, to analyze whether variations in CA - CA correlations were related to the observed hemisphere, we tested the constructed full model against a corresponding null model without the effect in question. In the same manner, we analyzed whether differences in dopamine- CA correlations were associated to phasic dopamine levels. All likelihood ratio tests were performed at a corrected $p \leq .05$ to account for multiple comparisons.

2.7 | Computational environment

Processing and visualization codes were written using the Python programming language, version 2.7 (Python Software Foundation, <https://www.python.org/>) and the open-source packages NumPy, SciPy (van der Walt, Colbert, & Varoquaux, 2011) and Matplotlib (Hunter, 2007). The statistical analysis was performed in R (R-Core-Team, 2016) using the packages lme4 (Bates, Machler, Bolker, & Walker, 2015), lsmeans (Lenth, 2016) and multcomp (Hothorn, Bretz, & Westfall, 2008).

3 | RESULTS

3.1 | Dopaminergic modulation of motocortical neural activity during speech production

As a first step, we examined temporal variations of neural potentials in the bilateral SMC, during real-life speaking compared to the resting state using iEEG recordings and neural simulations. We found that speech onset was associated with a down-regulation of voltages in the SMC, leading to decreased signal amplitudes during speaking (Figure 1a,b). Conversely, amplitudes were increased before speech onset as well as during pauses between words in sentences. The neural model demonstrated similar decreases in the magnitude of simulated neural

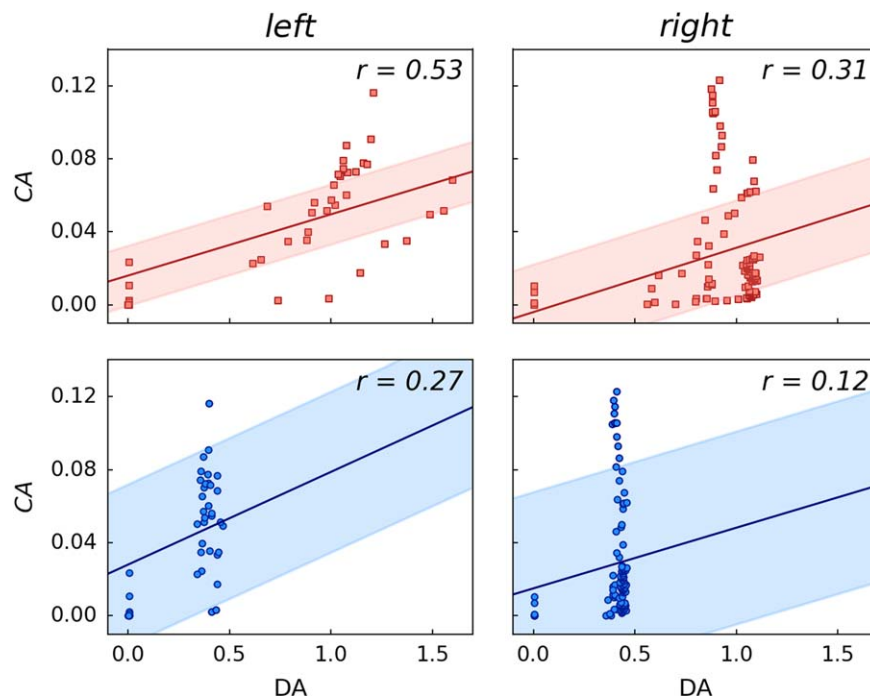


FIGURE 2 Correlation of simulated dopamine dynamics and cumulative differences of iEEG signal amplitudes. Shown are per-second values of $CA(t)$ and simulated dopamine (DA) corresponding to normal (top) and 50% reduced (bottom) phasic release across all recordings in the left and right hemisphere. Linear regression lines (solid) were computed based on averaged Fisher z-normalized correlation coefficients with shaded areas indicating corresponding standard deviations

potentials at the onset of dopamine release from the SNc to the SMC and dorsal putamen (Figure 1c).

To validate these findings, we performed a spectral analysis of both simulations and iEEG recordings. While iEEG recordings showed stronger low-frequency components than the simulations, both signals exhibited comparable power spectral densities across the examined frequency range, pointing to an underlying oscillatory pattern shared by both empirical data and computer model (Supporting information Figures S1, S2).

To examine the differences in simulated and empirical neural signals between the resting state and speaking, we computed the cumulative difference of amplitudes (CA) of both signals. We found consistently strong correlations between recordings and model output, which were independent of left/right hemisphere or tonic/phasic dopamine release ($r \geq .90$, $p < .0001$). Likelihood ratio tests of a LME model confirmed that correlations between simulated and empirical data were consistent and neither related to the observed hemisphere nor its interactions with phasic dopamine release ($p \geq .7$).

On the other hand, an assessment of the relationship between simulated dopamine release and empirical data as quantified by CA curves found a strong association to the levels of phasic dopamine release. Specifically, the interaction between dopamine dynamics in the model and iEEG signal envelopes was significantly related to changes in phasic dopamine levels (Fisher z-normalized mean correlations: left $r = .53$, right $r = .31$; $p = .01$), which was independent of the hemispheric side ($p = .57$) (Figure 2). While the simulated 50%-reduction of phasic dopamine levels decreased the correlations with empirical CA curves in both hemispheres, they nevertheless remained stronger in

the left than right hemisphere (Fisher z-normalized mean correlations: left $r = .27$, right $r = .12$) (Figure 2).

To further assess the dependence of hemispheric dominance effects on prevalent dopamine levels, we simulated increases and decreases of dopamine release in 10%-steps up to a 100% surplus and depletion of endogenous dopamine, respectively. We found that the correlation patterns between simulated dopamine dynamics and empirical CA curves were stable across a wide range of phasic dopamine release levels (from -80% to $+60\%$ of phasic dopamine release), which suggested stability of speech-induced laterality with respect to accessible endogenous dopamine (Figure 3). However, in case of overabundance or overdepletion of dopamine (increase above 70% or decrease below 10%), dopamine-CA correlation patterns became identical across hemispheres, indicating a loss of speech-related hemispheric dominance effects in the presence of abnormally high or abnormally low levels of dopamine release.

Taken together, these findings indicate that dopamine release directly modulated neural activity in the SMC, exerting left-hemispheric dominance.

3.2 | The effects of phasic dopamine release on hemispheric lateralization of neural networks during speech production

Based on empirical fMRI data acquired during speech production as well as neural simulations, likelihood ratio testing of LME models against null models showed that lateralization effects within both simulated and empirical fMRI data were condition-related and not by

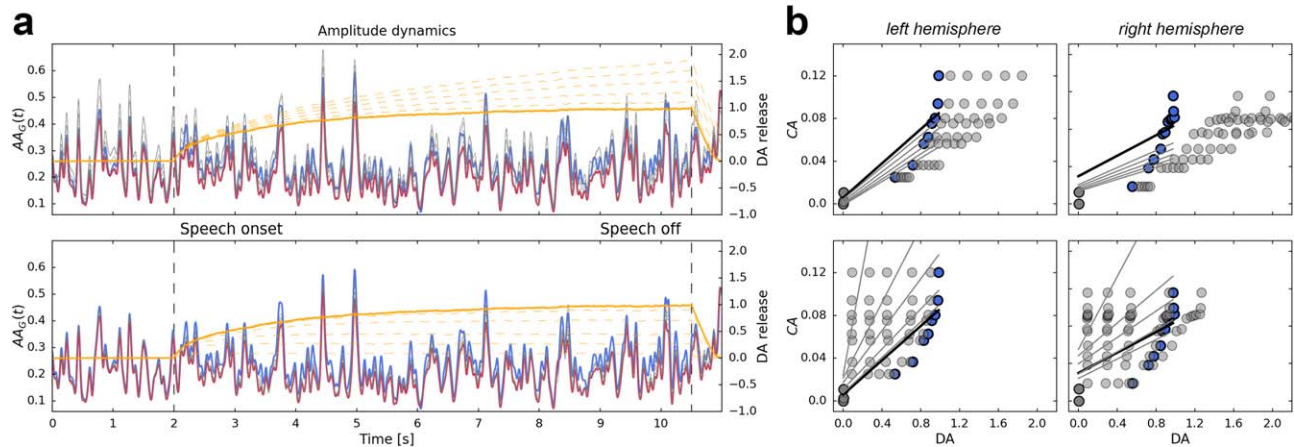


FIGURE 3 Neural activity dynamics in the speech motor cortex under varying phasic dopamine levels. (a) Temporal evolution of smooth envelopes AA_G corresponding to simulated resting state (blue) and speech production signals (red) in the left speech motor cortex under default phasic dopamine (DA) release (solid orange line) (compare to Figure 1). The upper panel illustrates increases in phasic dopamine (20% increments up to +100%) and the associated changes in AA_G (gray lines). The lower panel uses the same format to visualize the effect of decreases in phasic dopamine. (b) Per-second values of $CA(t)$ and simulated dopamine corresponding to normal phasic release (blue disks) in the left and right speech motor cortex with associated regression lines (black). The upper rows illustrate the effect of increased phasic dopamine levels (gray disks) on correlations (gray lines), the lower panel uses the same format to visualize the impact of lower phasic dopamine. Plots are based on the resting state and speech production segments shown in Figure 1. Similar patterns were observed in all other recordings

chance (both $p \leq .0007$). To assess lateralization effects at a whole-brain level, we computed a traditional laterality index, LI_1 , based on the summed total difference of activity across hemispheres (Seghier, 2008). In addition, we examined a task-based laterality index, LI_t , accounting for subject-specific baseline resting activity. The local hemispheric balance of speech-related regions was assessed by computing LI_t based on the connectivity from seeds in the bilateral SMC, SNc, and putamen using PPI analysis (Friston et al., 1997). Likelihood ratio tests of LME models found that laterality-index type and experimental condition (i.e., rest or speaking) were significantly interdependent (both $p \leq .02$). This finding implies that the observed laterality was affected both by the used index and the assessed condition. In support of our main hypothesis, both whole-brain laterality-indices, LI_t as well as LI_1 , did not show significant changes in hemispheric dominance between resting state and speech production in either fMRI data or neural simulations (all $p \geq .8$). However, PPI-based LI_t values showed pronounced lateralization of speech-related sub-networks. Specifically, when examining the hemispheric laterality of empirical fMRI recordings and simulations during speech production, we found that the SMC and putamen PPI-networks were characterized by strong left-hemispheric lateralization (all $p < .03$) (Figure 4).

One might argue that left-hemispheric lateralization of functional networks controlling speech production is based on left-hemispheric lateralization of underlying nigro-striatal and nigro-motocortical structural pathways. Although we showed previously that the SMC and putamen structural networks underlying speech production are bilaterally distributed (Simonyan et al., 2009; Simonyan et al., 2013), we nevertheless considered this possibility by simulating left-lateralized structural connectivity between the SNc and SMC as well as between the SNc and putamen. We found that enhanced structural connectivity

in the left hemisphere did not have a significant impact on functional network lateralization during speech production (all $p > .9$) (Figure 4). Compared to the resting state, local seed-based PPI-networks showed pronounced changes during speech production in the left hemisphere only (all $p < .05$) (Table 1). Notably, simulations based on artificially increased structural connectivity showed a distribution of PPI- LI_t values highly similar to original simulations (Figure 4). Enhancing structural nigral pathways did not affect the overall activation of SMC and putamen networks. However, the left hemisphere still showed significant deviations in activity compared to the corresponding resting state ($p \leq .048$ for both left SMC and putamen). While the left SMC network showed only trending differences between the resting state and speech production in the original simulations ($p = .076$), these differences became significant for unilaterally enhanced structural coupling. Nonetheless, SMC and putamen showed no statistically significant deviations from resting-state to speaking activity in the right hemisphere. Taken together, these findings suggest that structural changes in the simulated structural nigral pathways did not contribute to the left lateralization of functional networks during speaking.

4 | DISCUSSION

Our simulation-aided analysis of empirical data of high spatiotemporal resolution points to dopamine as a primary neuromodulator that underlies and drives left lateralization of neuronal activity and functional networks during speech production. Based on our modeling assumptions, nigral release of phasic dopamine spurred neural firing in the target regions of nigral afferents, that is, the putamen and SMC. This mechanism induced an increase in the oscillation frequency of excitatory

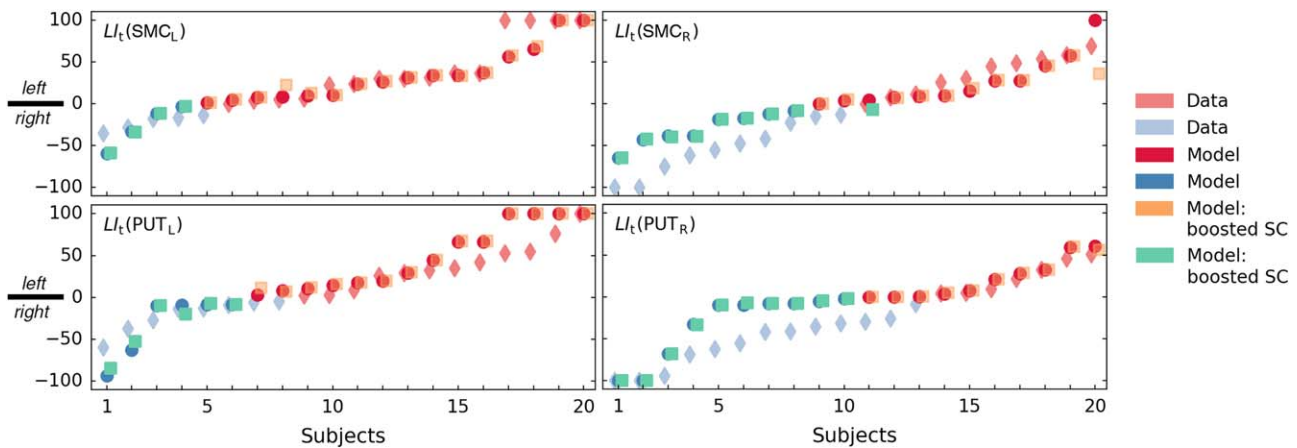


FIGURE 4 Lateralization patterns in empirical and simulated fMRI during speech production. Baseline corrected local PPI-based LI_t indices corresponding to seeds in bilateral speech motor cortex, $LI_t(SMC_L)$ and $LI_t(SMC_R)$, (top) and bilateral putamen, $LI_t(PUT_L)$ and $LI_t(PUT_R)$ (bottom). Orange and green markers indicate simulation values obtained using the original and artificially increased structural connectivity matrices, respectively. Values of whole-brain indices are shown in Supporting information Figure S3

neural membrane potentials in these regions, while simultaneously reducing associated voltage amplitudes. Specifically, the profile of amplitude dynamics in the left SMC, both in empirical and simulated data, suggested that neural potentials were characterized by an equivalent amplitude shift during speaking compared to the resting state (Figure 1 and Supporting information Figures S1, S2). In contrast, the nigral release of phasic dopamine had only a subtle effect on simulated neural dynamics in the right SMC. Right-hemispheric potentials had a far less distinct pattern, with speech-related amplitudes being close to or even larger than the corresponding resting-state values. Specifically,

amplitude dynamics in the right SMC did not show significant differences between the resting and speaking states.

Assessment of the relationship between simulated dopamine dynamics and empirical neural amplitude patterns in iEEG recordings revealed a complex interplay of lateralization profiles and phasic dopamine levels. At the cortical level, amplitude dynamics showed higher correlations with simulated dopamine time-courses in the left than right SMC, pointing to a mechanism by which dopamine selectively couples with and modulates neuronal activity in the left SMC during speech production. This observation at the cortical level is similar to our earlier report of left-lateralized striatal dopamine release and its coupling with neural activity in the left putamen, contributing to the left lateralization of striatal functional networks during speech production (Simonyan et al., 2013). Taken together, we suggest that dopamine release is likely a driver of speech-related left-hemispheric lateralization of neuronal activity via its direct modulatory effects on SMC and putamenal neural networks.

This assumption is further substantiated by our additional findings showing that both reductions and increases in phasic dopamine release levels (as low as 20% and as high as 60% of its normal level) lead to subsequent decreases and increases, respectively, in correlations between dopamine and neural amplitudes across both hemispheres, while preserving left-hemispheric lateralization. A similar finding was obtained with respect to striatal dopamine transporters (DATs) that showed preserved hemispheric lateralization despite a 46% decline in DATs linearly dependent on age (van Dyck et al., 2002). However, our study found pronounced changes in neural amplitude dynamics at extremely low (<10% of normal phasic dopamine release) and abnormally high (>70% of normal phasic dopamine release) endogenous dopamine levels, which effectively disrupted laterality of neural activity by equilibrating the pattern of dopamine/neural amplitude correlations across hemispheres while speaking. This finding provides evidence for clinical observations reporting vanishing lateralization of speech and language-related neural activity in schizophrenia (Ribolsi, Daskalakis,

TABLE 1 Summary statistics of laterality indices computed for simulated and empirical fMRI

	Data	Model	Model with boosted SC
$LI_1(r)$	-0.15 ± 0.24	-1.61 ± 4.22	-1.66 ± 4.26
$LI_1(s)$	0.33 ± 0.72	-1.27 ± 4.76	-1.26 ± 4.76
LI_t	8.53 ± 22.23	5.85 ± 24.52	6.01 ± 24.51
$LI_t(SMC_L)$	$25.63 \pm 42.57^*$	21.95 ± 37.96	$23.04 \pm 37.96^*$
$LI_t(SMC_R)$	-9.21 ± 51.39	3.21 ± 36.78	-0.34 ± 30.66
$LI_t(PUT_L)$	14.61 ± 38.19	$24.45 \pm 51.91^*$	$25.42 \pm 50.39^*$
$LI_t(PUT_R)$	$-26.24 \pm 45.01^*$	-6.49 ± 41.70	-6.44 ± 41.44

Values averaged across (virtual) subjects (mean \pm standard deviation) of L^1 -based indices $LI_1(r)$ and $LI_1(s)$ corresponding to resting state and speech production, respectively, whole brain baseline-corrected laterality index LI_t and local baseline-corrected PPI-based indices corresponding to seeds in bilateral speech motor cortex, $LI_t(SMC_L)$ and $LI_t(SMC_R)$, as well as bilateral putamen, $LI_t(PUT_L)$ and $LI_t(PUT_R)$, calculated for empirical data (first column), simulations (second column) and simulations based on unilaterally enhanced structural coupling between left SNc and SMC as well as left SNc and putamen (third column). Asterisks (*) indicate statistically significant differences compared to a zero-baseline level at $p \leq .05$ adjusted for multiple comparisons.

Siracusano, & Koch, 2014), which has been linked to hyperactive cortical dopamine neurotransmission (Brisch et al., 2014). Similarly, diminishing lateralization of neural activity in case of impaired phasic dopamine release has been implicated in patients with Parkinson's disease (Ventura et al., 2012; Batens et al., 2015), who experience speech motor problems from the early stage of their disorder. Thus, our findings provide a mechanistic explanation for the importance of phasic dopamine as a major neuromodulator of speech controlling circuitry in health and disease.

However, the effects of dopamine do not stop with its modulation and lateralization of cortical and striatal neuronal activity during speech production. Our study demonstrated that dopamine also induces the left-laterality of functional speech-controlling networks, which is more pronounced on a local small-scale level than in whole-brain networks. This is in line with recent studies from our group and others that reported bilaterally distributed whole-brain speech networks (Cogan et al., 2014; Silbert et al., 2014; Simonyan & Fuertinger, 2015) but a pronounced left-hemispheric lateralization of sub-networks that are part of the speech motor control system (Kell, Morillon, Kouneiher, & Giraud, 2011; Gehrig et al., 2012; Simonyan et al., 2013; Simonyan & Fuertinger, 2015). Here, we observed these lateralization effects not only in empirical iEEG and fMRI data but also in neural simulations, which speaks to the robustness and reproducibility of our findings across different experimental modalities. We found that dopamine-induced left-hemispheric lateralization of functional speech networks did not depend on the underlying neuroanatomy as enhancing the structural nigro-striatal and nigro-cortical pathways showed no significant effects on functional hemispheric dominance. Furthermore, when the connection strength underlying the left nigral pathways was doubled in simulations, the resulting changes in hemispheric dominance were negligible both at whole-brain and local small-scale levels. Collectively, these findings demonstrate a very stable hard wiring of the nigral pathways as an integral part of the speech motor control system while pointing to dopamine as an intrinsic modulator of functional speech networks.

4.1 | Limitations

A potential limitation is that the differences between the resting-state and speech production conditions are varied and oftentimes cannot be controlled for. However, it is important to keep in mind that when one starts speaking, normal speech usually occurs in complete, meaningful, and grammatically correct sentences rather than in disconnected and meaningless words, vowels, etc. Thus, in order to understand the complexity of neural networks controlling speech production, a realistic speech task ought to be used. That said, in our experiments, we controlled for speech variability by using a similar task of grammatically correct and meaningful English sentence production across all subjects. In addition, we devoted a separate study to specifically investigate the functional organization of a speech production network compared to a range of vocal and non-vocal control tasks of different complexity (Fuertinger et al., 2015). Specifically, we performed an in-depth assessment of brain activity patterns that were shared across tasks as

compared to the functional profile that was distinctly speech-specific. Following those investigations, the focus of this study was a detailed analysis of hemispheric dominance patterns emerging during speech production by contrasting empirical recordings with *in silico* simulations to assess the aspects of functional dependence that were not assessable otherwise and therefore not considered in our previous study. Thus, in the present context, resting-state brain activity was a natural baseline condition that was contrasted with a meaningful speech.

In order to assess the contribution of dopaminergic neurotransmission to speech-related functional lateralization patterns acting within a realistic anatomical framework, we relied on estimates of structural connections from diffusion MRI recordings. This approach is known to limit the degrees of freedom in a model's topology while simultaneously imposing only minimal anatomical assumptions, and is, therefore, widely used in the neural modeling community (Sanz-Leon, Knock, Spiegler, & Jirsa, 2015). Nonetheless, inferring connectional strength from diffusion tractography poses considerable methodological challenges, particularly, when assessing connections beyond major fiber tracts (Campbell & Pike, 2014; Thomas et al., 2014). Specifically, diffusion tractography does not differentiate between mono- and polysynaptic connections and is prone to false positive detections, particularly in areas of high fiber complexity (Jbabdi & Johansen-Berg, 2011; Reveley et al., 2015). This potentially limits the capabilities of applied tractography methods to model finer representations of the underlying neuroanatomical wiring patterns. However, even tract-tracing studies rely on the active axonal transport of tracers between neurons and are thus prone to noise corruption in case of simultaneous injections into multiple sites (Ypma & Bullmore, 2016). Thus, inferring inter-regional coupling strength from empirical measurements may reduce parameter space dimensionality at the cost of introducing an additional degree of uncertainty in the model.

It is also important to note that amplitude dynamics in empirical iEEG data generally attained larger values than those in neural simulations. This reflects the fact that rest-to-speech amplitude differences tended to be more pronounced in iEEG recordings, potentially due to two reasons. First, our inherent modeling assumption that dopamine is the major neuromodulator of brain activity during speech production neglected other relevant neurotransmitter functions. This approach, however, was taken intentionally given that our focus in the present study was to separate and quantify the explicit impact of dopaminergic modulation on the lateralization of neuronal activity and networks during real-life speech production as a complex behavior. Second, differences in experimental approaches to assess neural activity may have caused some discrepancies. Specifically, intracranial surface electrodes were implanted atop the pia mater to quantify electrical activity in underlying cortical tissue (Blanco et al., 2011), whereas our model simulated neural potentials was based on mean-field approximations of pyramidal cell populations (Fuertinger et al., 2014). Moreover, the pia mater has been suspected to act as a low-pass filter potentially amplifying slow oscillations while attenuating high-frequency components in iEEG recordings (Blanco et al., 2011). This effect might shape iEEG frequency spectra, which show power law relationships (Supporting information Figure S1). Conversely, at present, no mathematical closed-

form expression (including linear stochastic differential equations) is known to generate oscillations with a spectral density following a power law (Kaulakys, Ruseckas, Gontis, & Alaburda, 2006). While some phenomenological equations have been reverse-engineered from functions exhibiting an inversely proportional frequency spectrum, no widely accepted mechanistic model of these signals has been yet proposed (Wong, 2003). Thus, with the neurobiological underpinning of this effect still being unknown, we chose not to account for this phenomenon in our purely mechanistic neural population model. However, the generated simulations still showed a remarkable resemblance to empirical frequency spectra observed in iEEG recordings (Supporting information Figure S2) and high simulation-to-data correlations of amplitude dynamics (all $r \geq .9$).

4.2 | Conclusions and future work

Our findings indicate that dopaminergic neuromodulation is a key driver of functional but not structural left-hemispheric lateralization of neuronal activity and networks during speech production. Our mechanistic computational model successfully replicated lateralization patterns characteristic of empirical fMRI recordings and implied that dopamine plays a central role for the emergence of hemispheric dominance both at motocortical and striatal levels. The employed hybrid approach of computer simulations and empirical recordings further revealed that structural wiring strength of nigral pathways had a lesser, if any, impact on functional lateralization than phasic dopamine levels. These results shed light on the role of dopamine as a crucial neurotransmitter that shapes the functional hemispheric dominance of complex voluntary behaviors, such as human speech production.

It should, however, be noted that neural modeling efforts, such as the computational population model employed here, greatly simplify the neurobiological mechanisms being studied. While this may be done intentionally for modeling a particular behavior or anatomical link, this limitation should always be considered when interpreting the results of any simulation study. This further underscores the importance of continually improving and rigorously validating the mathematical models used to assess complex neurophysiological phenomena. In this context, a future study should analyze the impact of not only the function of dopamine but also gamma-aminobutyric acid (GABA), another major inhibitory neuromodulator in the speech motor control system. Further, subcortical feedback circuits and cerebellar components need to be modeled in greater detail in order to better reflect action selection and motor command execution.

ACKNOWLEDGMENTS

We thank Giovanni Battistella, PhD, for his assistance with processing fiber tractography data and Walter Hinds for assistance with electrode registration to MNI coordinates. This work was supported by the grants from the National Institute on Deafness and Other Communication Disorders, National Institutes of Health (R01DC011805) to KS.

CONFLICT OF INTEREST

The authors declare no competing interests.

ORCID

Kristina Simonyan  <http://orcid.org/0000-0001-7444-0437>

REFERENCES

- Baciu, M., Kahane, P., Minotti, L., Charnallet, A., David, D., Le Bas, J. F., & Segebarth, C. (2001). Functional MRI assessment of the hemispheric predominance for language in epileptic patients using a simple rhyme detection task. *Epileptic Disorders*, 3(3), 117–124.
- Batens, K., De Letter, M., Raedt, R., Duyck, W., Vanhoutte, S., Van Roost, D., & Santens, P. (2015). Subthalamic nucleus stimulation and spontaneous language production in Parkinson's disease: A double laterality problem. *Brain and Language*, 147, 76–84.
- Bates, D. M., Machler, M., Bolker, B. M., & Walker, S. (2015). Fitting linear mixed-effects models using lme4. *ArXiv e-print*.
- Battistella, G., Fuertinger, S., Fleysher, L., Ozelius, L. J., & Simonyan, K. (2016). Cortical sensorimotor alterations classify clinical phenotype and putative genotype of spasmodic dysphonia. *European Journal of Neurology*, 23(10), 1517–1527.
- Blanco, J. A., Stead, M., Krieger, A., Stacey, W., Maus, D., Marsh, E., ... Worrell, G. A. (2011). Data mining neocortical high-frequency oscillations in epilepsy and controls. *Brain*, 134(Pt 10), 2948–2959.
- Bouchard, K. E., Mesgarani, N., Johnson, K., & Chang, E. F. (2013). Functional organization of human sensorimotor cortex for speech articulation. *Nature*, 495(7441), 327–332.
- Breakspear, M., Terry, J. R., & Friston, K. J. (2003). Modulation of excitatory synaptic coupling facilitates synchronization and complex dynamics in a biophysical model of neuronal dynamics. *Network*, 14(4), 703–732.
- Brisch, R., Saniotis, A., Wolf, R., Bielau, H., Bernstein, H. G., Steiner, J., ... Gos, T. (2014). The role of dopamine in schizophrenia from a neurobiological and evolutionary perspective: Old fashioned, but still in vogue. *Frontiers in Psychiatry*, 5, 47.
- Campbell, J. S., & Pike, G. B. (2014). Potential and limitations of diffusion MRI tractography for the study of language. *Brain and Language*, 131, 65–73.
- Chang, E. F., Edwards, E., Nagarajan, S. S., Fogelson, N., Dalal, S. S., Canolty, R. T., ... Knight, R. T. (2011). Cortical spatio-temporal dynamics underlying phonological target detection in humans. *Journal of Cognitive Neuroscience*, 23(6), 1437–1446.
- Cogan, G. B., Thesen, T., Carlson, C., Doyle, W., Devinsky, O., & Pesaran, B. (2014). Sensory-motor transformations for speech occur bilaterally. *Nature*, 507(7490), 94–98.
- Cox, R. W. (1996). AFNI: Software for analysis and visualization of functional magnetic resonance neuroimages. *Computers and Biomedical Research*, 29(3), 162–173.
- Desikan, R. S., Segonne, F., Fischl, B., Quinn, B. T., Dickerson, B. C., Blacker, D., ... Killiany, R. J. (2006). An automated labeling system for subdividing the human cerebral cortex on MRI scans into gyral based regions of interest. *NeuroImage*, 31(3), 968–980.
- Dykstra, A. R., Chan, A. M., Quinn, B. T., Zepeda, R., Keller, C. J., Cormier, J., ... Cash, S. S. (2012). Individualized localization and cortical surface-based registration of intracranial electrodes. *NeuroImage*, 59(4), 3563–3570.

- Fischl, B., Sereno, M. I., Tootell, R. B., & Dale, A. M. (1999). High-resolution intersubject averaging and a coordinate system for the cortical surface. *Human Brain Mapping*, 8(4), 272–284.
- Flinker, A., Korzeniewska, A., Shestiyuk, A. Y., Franaszczuk, P. J., Dronkers, N. F., Knight, R. T., & Crone, N. E. (2015). Redefining the role of Broca's area in speech. *Proceedings of the National Academy of Sciences of the United States of America*, 112(9), 2871–2875.
- Freeman, W. J. (2005). Origin, structure, and role of background EEG activity. Part 3. Neural frame classification. *Clinical Neurophysiology*, 116(5), 1118–1129.
- Friston, K. J., Buechel, C., Fink, G. R., Morris, J., Rolls, E., & Dolan, R. J. (1997). Psychophysiological and modulatory interactions in neuroimaging. *NeuroImage*, 6(3), 218–229.
- Frost, J. A., Binder, J. R., Springer, J. A., Hammeke, T. A., Bellgowan, P. S. F., Rao, S. M., & Cox, R. W. (1999). Language processing is strongly left lateralized in both sexes - Evidence from functional MRI. *Brain*, 122, 199–208.
- Fuertinger, S., Horwitz, B., & Simonyan, K. (2015). The functional connectome of speech control. *PLoS Biology*, 13(7), e1002209.
- Fuertinger, S., Zinn, J. C., & Simonyan, K. (2014). A neural population model incorporating dopaminergic neurotransmission during complex voluntary behaviors. *PLoS Computational Biology*, 10(11), e1003924.
- Gehrig, J., Wibral, M., Arnold, C., & Kell, C. A. (2012). Setting up the speech production network: How oscillations contribute to lateralized information routing. *Frontiers in Psychology*, 3, 169.
- Glover, G. H., Li, T. Q., & Ress, D. (2000). Image-based method for retrospective correction of physiological motion effects in fMRI: RETROICOR. *Magnetic Resonance in Medicine*, 44(1), 162–167.
- Gow, D. W., Jr., Keller, C. J., Eskandar, E., Meng, N., & Cash, S. S. (2009). Parallel versus serial processing dependencies in the perisylvian speech network: A Granger analysis of intracranial EEG data. *Brain and Language*, 110(1), 43–48.
- Hagmann, P., Cammoun, L., Gigandet, X., Meuli, R., Honey, C. J., Wedeen, V. J., & Sporns, O. (2008). Mapping the structural core of human cerebral cortex. *PLoS Biology*, 6(7), e159.
- Hothorn, T., Bretz, F., & Westfall, P. (2008). Simultaneous inference in general parametric models. *Biometrical Journal*, 50(3), 346–363.
- Hull, R., & Vaid, J. (2006). Laterality and language experience. *Laterality*, 11(5), 436–464.
- Hunter, J. D. (2007). Matplotlib: A 2D graphics environment. *Computing in Science & Engineering*, 9(3), 90–95.
- Jbabdi, S., & Johansen-Berg, H. (2011). Tractography: where do we go from here?. *Brain Connectivity*, 1(3), 169–183.
- Jo, H. J., Saad, Z. S., Simmons, W. K., Milbury, L. A., & Cox, R. W. (2010). Mapping sources of correlation in resting state fMRI, with artifact detection and removal. *NeuroImage*, 52(2), 571–582.
- Kaulakys, B., Ruseckas, J., Gontis, V., & Alaburda, M. (2006). Nonlinear stochastic models of 1/f noise and power-law distributions. *Physica A*, 365, 217–221.
- Kell, C. A., Morillon, B., Kouneihir, F., & Giraud, A. L. (2011). Lateralization of speech production starts in sensory cortices—a possible sensory origin of cerebral left dominance for speech. *Cerebral Cortex*, 21(4), 932–937.
- Lachaux, J. P., Jerbi, K., Bertrand, O., Minotti, L., Hoffmann, D., Schoendorff, B., & Kahane, P. (2007). A blueprint for real-time functional mapping via human intracranial recordings. *PLoS One*, 2(10), e1094.
- Lenth, R. V. (2016). Least-squares means: The R package lsmeans. *Journal of Statistical Software*, 69(1), 1–33.
- Llorens, A., Trebuchon, A., Liegeois-Chauvel, C., & Alario, F. X. (2011). Intra-cranial recordings of brain activity during language production. *Frontiers in Psychology*, 2, 375.
- Newman, S. D., Twieg, D. B., & Carpenter, P. A. (2001). Baseline conditions and subtractive logic in neuroimaging. *Human Brain Mapping*, 14(4), 228–235.
- Price, C. J. (2012). A review and synthesis of the first 20 years of PET and fMRI studies of heard speech, spoken language and reading. *NeuroImage*, 62(2), 816–847.
- R-Core-Team. (2016). *R: A language and environment for statistical computing*. Vienna, Austria: R Foundation for Statistical Computing.
- Reveley, C., Seth, A. K., Pierpaoli, C., Silva, A. C., Yu, D., Saunders, R. C., ... Ye, F. Q. (2015). Superficial white matter fiber systems impede detection of long-range cortical connections in diffusion MR tractography. *Proceedings of the National Academy of Sciences of the United States of America*, 112(21), E2820–E2828.
- Ribolsi, M., Daskalakis, Z. J., Siracusano, A., & Koch, G. (2014). Abnormal asymmetry of brain connectivity in schizophrenia. *Frontiers in Human Neuroscience*, 8, 1010.
- Sanz-Leon, P., Knock, S. A., Spiegler, A., & Jirsa, V. K. (2015). Mathematical framework for large-scale brain network modeling in the virtual brain. *NeuroImage*, 111, 385–430.
- Seghier, M. L. (2008). Laterality index in functional MRI: Methodological issues. *Magnetic Resonance Imaging*, 26(5), 594–601.
- Silbert, L. J., Honey, C. J., Simony, E., Poeppel, D., & Hasson, U. (2014). Coupled neural systems underlie the production and comprehension of naturalistic narrative speech. *Proceedings of the National Academy of Sciences of the United States of America*, 111(43), E4687–E4696.
- Simonyan, K. (2014). The laryngeal motor cortex: Its organization and connectivity. *Current Opinion in Neurobiology*, 28, 15–21.
- Simonyan, K., & Fuertinger, S. (2015). Speech networks at rest and in action: Interactions between functional brain networks controlling speech production. *Journal of Neurophysiology*, 113(7), 2967–2978.
- Simonyan, K., Herscovitch, P., & Horwitz, B. (2013). Speech-induced striatal dopamine release is left lateralized and coupled to functional striatal circuits in healthy humans: A combined PET, fMRI and DTI study. *NeuroImage*, 70, 21–32.
- Simonyan, K., Ostuni, J., Ludlow, C. L., & Horwitz, B. (2009). Functional but not structural networks of the human laryngeal motor cortex show left hemispheric lateralization during syllable but not breathing production. *Journal of Neuroscience*, 29(47), 14912–14923.
- Spreer, J., Arnold, S., Quiske, A., Wohlfarth, R., Ziyeh, S., Altenmuller, D., ... Schumacher, M. (2002). Determination of hemisphere dominance for language: Comparison of frontal and temporal fMRI activation with intracarotid amytal testing. *Neuroradiology*, 44(6), 467–474.
- Strauss, E., Kosaka, B., & Wada, J. (1983). The neurobiological basis of lateralized cerebral function. A review. *Human Neurobiology*, 2(3), 115–127.
- Taylor, P. A., & Saad, Z. S. (2013). FATCAT: (an efficient) functional and tractographic connectivity analysis toolbox. *Brain Connectivity*, 3(5), 523–535.
- Thomas, C., Ye, F. Q., Irfanoglu, M. O., Modi, P., Saleem, K. S., Leopold, D. A., & Pierpaoli, C. (2014). Anatomical accuracy of brain connections derived from diffusion MRI tractography is inherently limited. *Proceedings of the National Academy of Sciences of the United States of America*, 111(46), 16574–16579.
- Towle, V. L., Yoon, H. A., Castelle, M., Edgar, J. C., Biassou, N. M., Frim, D. M., ... Kohrman, M. H. (2008). ECoG gamma activity during a language task: Differentiating expressive and receptive speech areas. *Brain*, 131(Pt 8), 2013–2027.

- van der Walt, S., Colbert, S. C., & Varoquaux, G. (2011). The NumPy Array: A structure for efficient numerical computation. *Computing in Science & Engineering*, 13(2), 22–30.
- van Dyck, C. H., Seibyl, J. P., Malison, R. T., Laruelle, M., Zoghbi, S. S., Baldwin, R. M., & Innis, R. B. (2002). Age-related decline in dopamine transporters: Analysis of striatal subregions, nonlinear effects, and hemispheric asymmetries. *The American Journal of Geriatric*, 10(1), 36–43.
- Ventura, M. I., Baynes, K., Sigvardt, K. A., Unruh, A. M., Acklin, S. S., Kirsch, H. E., & Disbrow, E. A. (2012). Hemispheric asymmetries and prosodic emotion recognition deficits in Parkinson's disease. *Neuropsychologia*, 50(8), 1936–1945.
- Welch, P. (1967). The use of the fast Fourier transform for the estimation of power spectra: A method based on time averaging over short, modified periodograms. *IEEE Transactions on Audio and Electroacoustics*, 15, 70–73.
- Wong, H. (2003). Low-frequency noise study in electron devices: Review and update. *Microelectronics Reliability*, 43, 585–599.
- Ypma, R. J., & Bullmore, E. T. (2016). Statistical analysis of tract-tracing experiments demonstrates a dense, complex cortical network in the mouse. *PLoS Computational Biology*, 12(9), e1005104.

SUPPORTING INFORMATION

Additional Supporting Information may be found online in the supporting information tab for this article.

How to cite this article: Fuertinger S, Zinn JC, Sharan AD, Hamzei-Sichani F, Simonyan K. Dopamine drives left-hemispheric lateralization of neural networks during human speech. *J Comp Neurol*. 2018;526:920–931. <https://doi.org/10.1002/cne.24375>